Metal-Organic Frameworks (MOFs) Composed of (Triptycenedicarboxylato)zinc

Sergei Vagin,[a,b] Anna Ott,[a,b] Hans-Christoph Weiss,[c] Alexander Karbach,[c] Dirk Volkmer,[b] and Bernhard Rieger*[a,b]

Introduction

In recent years, the interest in employing 3D metal-organic frameworks (MOFs) as micro-porous materials has grown immensely due to the high number of potential applications in materials science and industrial technologies. Among their useful properties, nonlinear optical activity,[1] sensing,[2] selective sorption and selective catalytic activity,[3] storage of gases, in particular H_2,[4] etc. can be mentioned. The versatility of the attractive features manifested by this class of materials is mostly due to the wide possibilities for altering and fine-tuning their structures which can be achieved by matching the organic polydentate linker (L) and/or metal-containing secondary building block (SBU).[5]

Up to now, most investigations on MOFs were focused on applications based around gas storage or selective sorption. Regarding hydrogen sorption, the strategies proposed to increase hydrogen uptake were aimed both at modification of the organic linker structures, e.g. by extending their aromatic moieties,[6a] as well as at development of new MOF topologies and optimisation of the pore size and geometry.[6b–6d]

The vast empirical knowledge in the field of metal-organic frameworks shows that the constitution of SBUs and the final MOF topology adopted upon self-assembly are not always unambiguously predictable and controllable. In general, they are very much dependent on the structures and properties of organic ligands as well as on the conditions of synthesis and the Zn-containing frameworks are no exception. The simultaneous formation of coordination polymers with distinct structures from the same components (supramolecular isomers) is often the case.[7] Using the same ligand, such as terephthalic acid, might lead to different MOF topologies upon coordinating to Zn ions (starting, for example, from $Zn(NO_3)_2{\cdot}4H_2O$, under distinctive reaction conditions). Thus, topologically different MOFs comprising tetranuclear $\{Zn_4O\}$ units (MOF-5),[8a] trinuclear $\{Zn_3\}$[8b] as well as dinuclear paddlewheel $\{Zn_2\}$ units[8c] have been prepared with this dicarboxylic acid. The partial metal exchange of Zn by divalent ions of, for example, Ni, Co or Cd may also lead to completely rearranged framework structures instead of the expected architectures.[9] On the other hand, a wide range of MOFs based on tetranuclear $\{Zn_4O\}$ coordination units (CUs) could be obtained simply by adopting the common synthetic procedure for MOF-5 (IRMOF-1) but, instead, utilising structurally different ditopic aromatic carboxylato groups linkers.[10a] In this respect, comprehensive insights into the fundamental principles driving the network assembly in the early stages of MOF synthesis would be of immense theoretical and practical interest.

Here we report two novel MOFs utilising triptycenedicarboxylic acid (H_2TDC) and zinc which can be prepared under the reaction conditions that normally lead to a pcu-net[10b] based on $\{Zn_4O\}$ units as, for example, in MOF-5. However, instead of the anticipated framework, two novel coordination polymers were obtained which are constructed

[a] WACKER-Lehrstuhl für Makromolekulare Chemie, Technische Universität München,
Lichtenbergstraße 4, 85747 Garching, Germany
Fax: +49-89-289-13562,
E-mail: rieger@tum.de
[b] Institut für Anorganische Chemie II, Universität Ulm,
Albert-Einstein-Allee 11, 89081 Ulm, Germany
[c] Bayer Industry Services GmbH & Co OHG,
Building Q 18, 51368 Leverkusen, Germany

from paddlewheel SBUs with three or four blades, respectively.[10c] To the best of our knowledge, no coordination compounds of H_2TDC have been reported up to now in the Cambridge Structural Database and the new coordination networks described here are the first examples of MOFs with this bulky dicarboxylato ligand.

Results and Discussion

The intention of utilising a triptycene dicarboxylato group instead of the more common terephthalato ligand can be rationalised as the attempt to create the additional contact surface for the adsorption of small guest molecules in modified MOFs. For example, increasing void diameters or volumes in MOF structures does not automatically give rise to a positive impact on hydrogen absorption and a less porous network such as an interpenetrating network structure might in fact be desired for the more effective hydrogen physisorption at low temperatures and pressures.[4b,6] According to another report, a fourfold interpenetrated $\{Zn_4O\}$ MOF constructed from sterically demanding aromatic linkers possesses a six times lower pore volume than MOF-5 although its hydrogen storage capacity (48 bar, room temperature) is comparable to that of MOF-5 under the same conditions.[11] Encouraged by these studies, we considered 9,10-triptycenedicarboxylic acid as a suitable bis(bidentate) ligand to design new MOFs for the sorption of small molecules, e.g. H_2. Indeed, we anticipated that three benzene rings arranged at 120° angles to one another could increase the interaction energy of an H_2 molecule with the aromatic π system of the ligand by means of a partial "sandwiching" effect, i.e. simultaneous interaction of H_2 with two benzene rings of the three V-shaped moieties, as observed, for example for I_2 and Ne.[12]

9,10-Triptycenedicarboxylic acid (H_2TDC), as shown in Scheme 1, was synthesised according to a route proposed in a patent.[13] The overall yield of the product based on anthracene was ca. 30% but this could still be optimised thereby facilitating a large scale preparation of H_2TDC. The compound was then allowed to react with $Zn(NO_3)_2 \cdot 4H_2O$ or $Zn(NO_3)_2 \cdot 6H_2O$ under solvothermal conditions in diethylformamide (DEF) to give polycrystalline precipitates.

The IR spectra of the resultant solids clearly indicated a complete conversion of H_2TDC into the corresponding dicarboxylato derivative (TDC). The C=O stretching vibration of the carboxylic acid groups at 1705 cm^{-1} in H_2TDC underwent a low-frequency shift to approximately 1640 cm^{-1} and the absorption in the region from 2500 to 3000 cm^{-1} ascribed to the O–H stretching mode in the hydrogen bonded carboxylic acid groups disappeared. Additionally, new bands typical for aliphatic C–H stretching modes in the IR spectra of the vacuum- and temperature-dried materials were observed at 2875–2990 cm^{-1}, indicating the presence of DEF in the isolated MOF compound.

Crystals of different sizes and morphologies (see Figure 1) were found in the precipitated materials. Their relative abundances are strongly dependent on the synthetic conditions, e.g. reaction temperature and time, as well as on the reactant ratios. Small polygonal platelets (e.g. tetragonal, hexagonal or octagonal) were observed both by light and scanning electron microscopy (SEM). Relatively large irregularly shaped crystals such as intergrown columns, blocks or thick spikes were also formed, sometimes as the major products, which are completely covered by microplatelets (see Figure S1 in the Supporting Information). Additionally, regular hexagonal columns and morphologically related crystals were revealed in some synthetic batches.

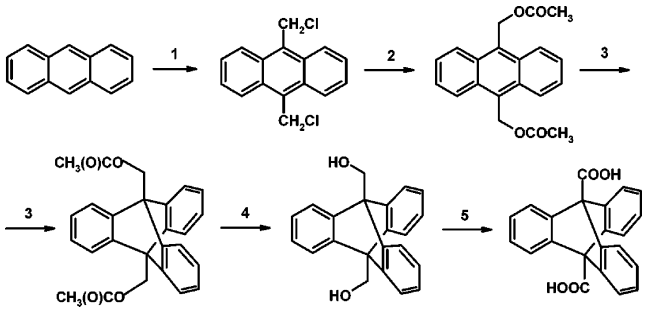

Scheme 1. Synthesis of 9,10-triptycenedicarboxylic acid (H_2TDC): 1. $[CH_2O]_n$, $HCl_{(g)}$, dioxane; 2. NaOAc, HOAc; 3. anthranilic acid, isopentyl nitrite, dimethoxyethane, maleic anhydride, $KOH_{(aq)}$; 4 KOH, MeOH, H_2O; 5. CrO_3, $H_2SO_{4(aq)}$, acetone.

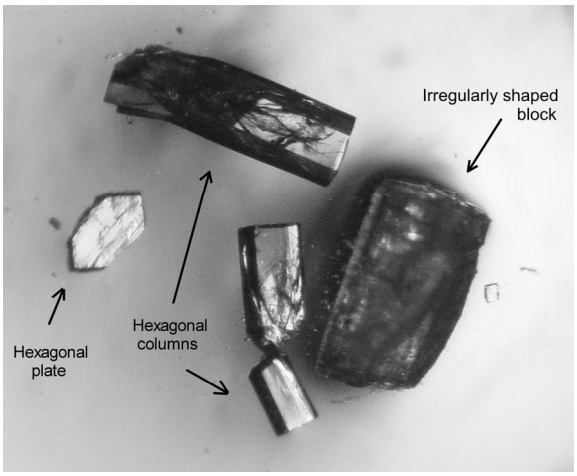

Figure 1. Polarised light optical micrograph showing different types of crystals formed during the synthesis of (triptycenedicarboxylato)zinc MOFs in DEF solvent.

The single-crystal X-ray diffraction (SXRD) analysis of a hexagonal plate (Figure 1) picked from one of the synthetic batches allowed us to formulate its structure as a 2D MOF (TDC-MOF-1) with the composition [Zn(TDC)(DEF)]. This 2D coordination polymer is formed by slightly distorted paddlewheel secondary building units (see parts a and b of Figure 2). The distance of 2.93 Å between two zinc ions in the CUs of TDC-MOF-1 is typical for zinc paddlewheel complexes bridged by four carboxylic groups in a *syn-syn* mode.[14a] The compound crystallises in the monoclinic space group *C*2/*c*. The planar tetragonal structural fragment spanned between points ABCD of TDC-MOF-1

consisting of four di-zinc paddlewheel units linked by four TDCs $\{(Zn_2)_4(\mu\text{-TDC})_4\}$ (see Figure 2, c) forms planar 4^4-tiling layers parallel to the *ab* plane of the crystal lattice. This structural element has a geometry of a rhombus which results in a close contact between adjacent triptycene units with an angle of approximately 84.2° at the A and C vertices. Such a deviation from a regular square geometry in the $\{(Zn_2)_4(\mu\text{-TDC})_4\}$ layers might be due to the gain in interaction energy resulting from the "gearing" (CH–π and π–π) interaction in two pairs of triptycene three-blade rotors at the A and C vertices with the shortest C···C distance between the interacting blades amounting to 3.27 Å. No specific interactions were found between the 2D layers in the crystal lattice. The layers seem to assemble only by means of van der Waals interactions between the DEF residues of neighbouring 2D sheets or between the DEF "tails" of one sheet and the triptycene V-shaped "clefts" of another neighbouring sheet (see part d of Figure 1, the marked distances are in the range 3.4–3.8 Å). A very weak C–H···O hydrogen bond can, however, also be postulated as existing between the methyl groups of DEF in one layer and the carboxylato groups in another layer with an H···O distance of 2.5–2.8 Å.

As mentioned above, the crystal platelets described here are not the only type of crystals formed in DEF at 110–120 °C. Immediate analysis of the resultant materials by powder X-ray diffraction (PXRD) and SEM allows us to suggest the simultaneous formation of several MOF phases at different ratios strongly depending on the conditions of synthesis (see Figures S1–S3 in the Supporting Information). PXRD patterns of the materials, however, changed upon drying or workup, probably due to the loss of occluded solvent molecules. Finally, the synthesised products become converted into TDC-MOF-1, for example upon drying at elevated temperature in vacuo, as their PXRD patterns show a rather good agreement with that calculated from the single crystal analysis data, although the broadening of the experimental reflection peaks might indicate some loss of product crystallinity upon fast drying (Figure S2 in the Supporting Information). The shapes of the large crystals as well as of the small platelets remain unchanged after drying, though their exfoliation could be observed with SEM. Exfoliation was also observed for the synthesised plate-like crystals but it is not clear whether this comes from drying out under the vacuum conditions of SEM (10 to 40 Pa) or whether this is a defect introduced during crystal growth (compare Figures S1 and S3 in the Supporting Information).

The elemental analysis of the dried bulk product fits satisfactorily with the [Zn(TDC)(DEF)] composition. It is reasonable to suppose that the major phases in the synthesised material are composed of the stable 2D $[Zn(TDC)(DEF)]_\infty$ layers which are separated from each other by occluded solvent molecules in different manners (e.g. with different offsets and distances depending on the phase) and which build TDC-MOF-1 upon solvent removal. Additionally, the layered structures based on trinuclear zinc units can also be supposed in the samples and this could transform over a certain period into TDC-MOF-1 as well. Similar processes in other MOFs, e.g. self-assembled from terephthalic acid and zinc, are already known.[14a,14c]

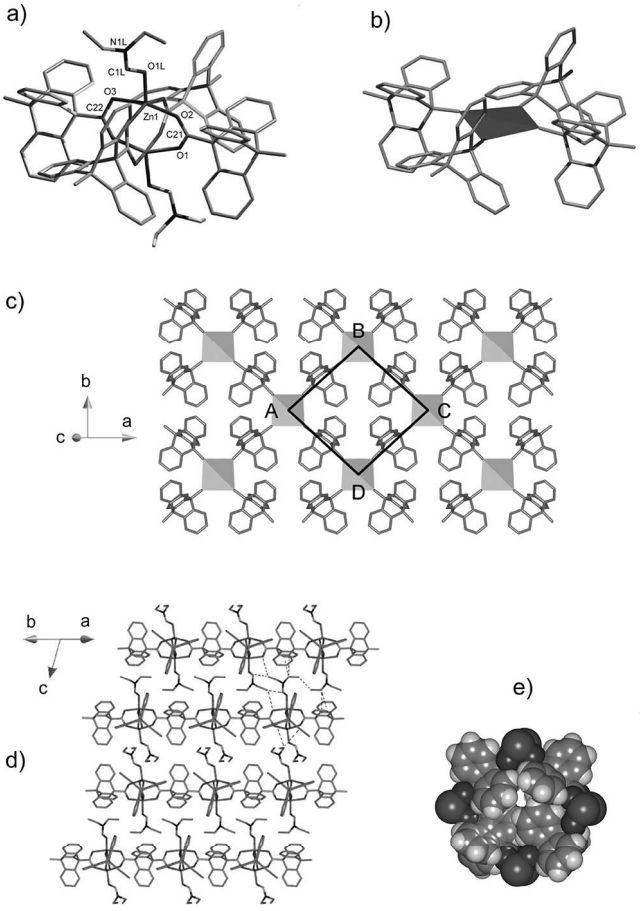

Figure 2. Structural features of TDC-MOF-1 (hydrogen atoms are sometimes omitted for clarity): four-bladed dinuclear zinc paddlewheel CU (a) and its schematic representation by a distorted rectangle (b); 2D layer of interlinked paddlewheel units viewed at normal direction to the *ab* plane (c); stacking of 2D layers viewed along the [1,1,0] direction (d) and space-filling representation of the rhombic structural element ABCD indicated in (c) which demonstrates the dense arrangement of triptycene units within each 2-D layer (e).

The statements above are also supported by thermogravimetric analysis. Although no occluded solvent molecules placed at crystallographically defined positions were found in the crystal structure of TDC-MOF-1, TGA data of air-dried bulk material indicates the presence of up to 10% of noncoordinated water and DEF in various ratios depending on the synthetic batch and this might explain the irreproducibility and low accuracy of the elemental analysis for the synthesised product. The loss of occluded molecules can be observed as two rather sharp steps appearing in the TGA curve at temperatures ranging from 90 to 110 °C and from 170 to 190 °C. TDC-MOF-1 dried at 150 °C in vacuo does not show any weight loss up to 270 °C, at which temperature the coordinated DEF is volatilised in two subsequent steps (see Figure S7 in the Supporting Information and

Exp. Sect.). Approximately 13.5% weight loss may be observed during the first step (up to 360 °C) which is somewhat higher than calculated for the split of one DEF molecule per dinuclear zinc coordination unit (10%). Complete removal of coordinated DEF molecules is achieved above 400 °C, followed by the decomposition of coordinated TDC units. Investigation of the porosity of dried TDC-MOF-1 by recording BET isotherms shows a very low "apparent surface" (ca. 5 $m^2 g^{-1}$) which could be expected in light of its dense packing arrangement.

The general yield of bulk TDC-MOF-1 in the synthesis at 120 °C drops upon increasing the $Zn(NO_3)_2$ to H_2TDC ratio (see Table 1). An additional prolongation of the reaction time leads to competitive formation of crystals having the shape of regular hexagonal columns, these being the compound TDC-MOF-2 (see Figure 1). After having filtered off the plate-like crystals and blocks formed within the first 24 h, hexagonal columns continuously formed from the remaining reaction mixture as the sole product containing TDC. However, there was some contamination consisting of a yellowish often amorphous powder with a very high zinc content according to EDX measurements (see Figures S4 and S5 in the Supporting Information). This impurity could be zinc oxide/hydroxide or (formato)zinc and the relative amount of it was especially high with an increasing amount of zinc salt relative to H_2TDC and this is quite understandable. The largest hexagonal columns were formed when the ratio of zinc salt to H_2TDC was the highest but they quickly turned opaque and became fragile already during synthesis. TDC-MOF-2 was also formed nearly solely when the solutions of reacting components were separately preheated to 120 °C before being mixed. The resultant hexagonal columns, however, feature abundant macroscopic defects due to the high rate of crystal growth (see Figure S6a in the Supporting Information). Contrary to what was mentioned above, an increase in the Zn to TDC ratio leads to finer crystals in this case due to the slower formation. Nevertheless, SXRD analysis of the hexagonal columns from different batches indicated their identity.

The structure of TDC-MOF-2 could be reasonably solved and refined in the trigonal crystal system with the space group $P\bar{3}$ (no. 147) and in the hexagonal crystal system with the space group *P6/m* (no. 175) but the final structural refinement was accomplished in *P6/m*. The X-ray structure analysis shows that the crystals are composed from dinuclear zinc CUs symmetrically linked by three TDC units ("three-bladed" paddlewheels[10c]) to form layers. Additionally, each paddlewheel unit has two axially coordinated TDCs which crosslink the layers and extend the structure into three dimensions. This framework can be thus considered as a pillared 6^3 net or as a distorted 5-connected bnn-net.[10b] However, two different coordination modes of axial TDCs can be distinguished (Figure 3). The unit cell of TDC-MOF-2 contains eight paddlewheel clusters, two of which have apical TDC ligands coordinated in a slightly distorted bidentate (chelating) mode with disorder of the carboxylato group about the vertical threefold symmetry axis (see part c of Figure 3, type-II clusters). The carbon atom C48 of the apical carboxylato group and both zinc ions in such a cluster are positioned on a common axis. However, hard restraints had to be applied for modelling this cluster in order to obtain reasonable Zn2–O7′ and Zn2–O7 distances (1.98 and 2.03 Å, respectively), probably as a consequence of the disorder and high diffuse electron density. Apical TDCs in the remaining six dinuclear units (type I clusters) coordinate by the carboxylic groups in a monodentate *syn* mode (the Zn1–O5 and Zn1–O6 distances are 1.94 and 2.67 Å, respectively, and the Zn1–Zn1–C43 angle is 164.5°, Figure 3, a) which leads to the tetracoordinated zinc ions.

The (triptycenedicarboxylato)zinc framework in TDC-MOF-2 possesses two different types of linear channels with different shapes and sizes (see parts e and f in Figure 3) and a total potential solvent accessible volume (PSAV) of 51% calculated with PLATON.[15] Twelve DEF molecules per layer segment could be located in the "pocket" of larger (regular hexagonal, PSAV = 20%) channels and reasonably resolved by SXRD analysis. Each DEF molecule interacts with a neighbouring triptycene unit of the 2D layer in such a way that one methyl group of DEF fits into the triptycene cleft with distances of 3.57 Å and 3.71 Å to the corresponding benzo-rings as shown in Figure 4. The methylene group of another ethyl substituent in the DEF molecule appears

Table 1. Formation of MOFs in DEF (20 mL) using different ratios of $Zn(NO_3)_2$ to H_2TDC at 120 °C.

Mass of $Zn(NO_3)_2 \cdot 6H_2O$ / mg	Mass of H_2TDC / mg	Ratio of reagents	Duration of reaction / h	Mass of precipitate formed / mg	Type of product
297	344	1:1	0–24	384	TDC-MOF-1
			24–72	6	TDC-MOF-1 + -2
892	344	3:1	0–24	281	TDC-MOF-1
			24–72	237	TDC-MOF-2 + impurities
1190	344	4:1	0–24	161	TDC-MOF-1
			24–72	430	TDC-MOF-2 + impurities
1487	344	5:1	0–24	71	TDC-MOF-1 + -2 (as junctions)
			24–72	706	TDC-MOF-2 + impurities
1785	344	6:1	0–24	–	–
			24–72	776	TDC-MOF-2 + impurities
2677	344	9:1	0–24	69	TDC-MOF-1 (traces) + impurity
			24–72	1030	TDC-MOF-2 + impurities

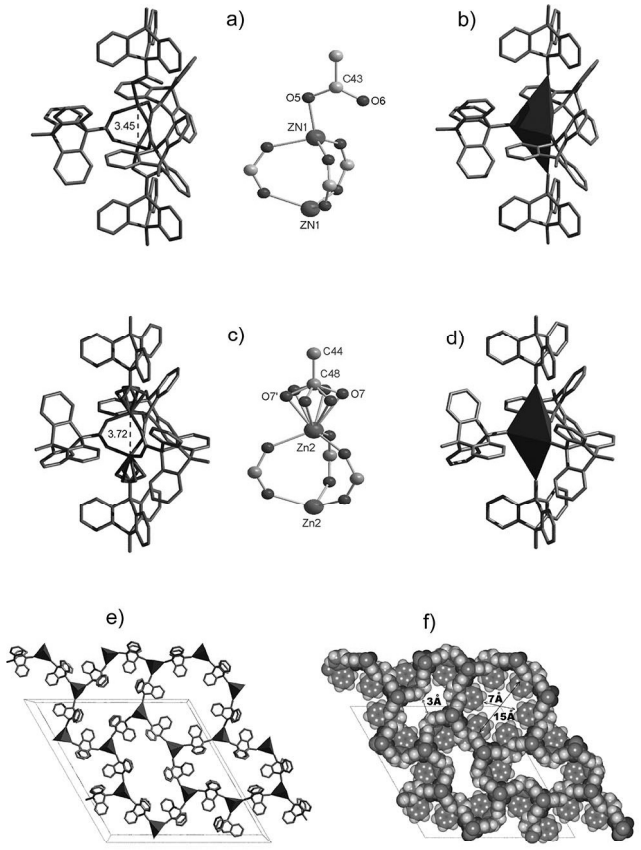

Figure 3. Structures of paddlewheel CUs in TDC-MOF-2 (a: type I cluster; c: type II cluster), their representation with polyhedra (b, d) and assembly into a layer (e, perspective view normal to the *ab* plane, axial TDC ligands are not shown; f, space-filling representation with axial TDCs). Solvent molecules are omitted for clarity. Distances shown in (f) are between the van der Waals surfaces of the carbon atoms.

to be in the proximity of the triptycene cleft which interlinks the layers (the shortest CH_2–C_{Ar} distance is 3.63 Å). The carbonyl groups of the DEF molecules are turned towards the centre of the channel and form a hydrogen-bonding network (see Figure 4) with another guest species

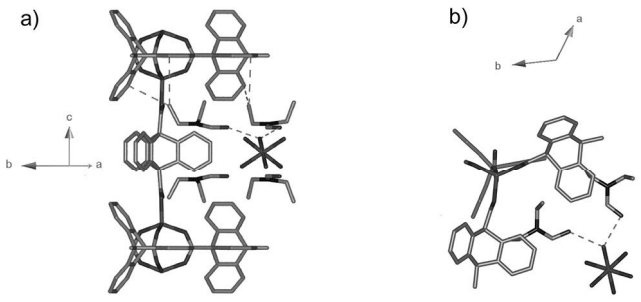

Figure 4. Structural fragment of TDC-MOF-2 showing the interactions between the guest species in the hexagonal channel: a) view along the *ab* plane of the unit cell; b) view along the *c* axis. Hydrogen atoms and the disorder of the hexaaquazinc complex are not shown for clarity.

located on a six-fold symmetry axis which was resolved as a disordered and slightly distorted octahedral hexaaquazinc(II) complex (one half per elementary cell). The observed Zn–O distances in this complex are 1.96 Å and the O–Zn–O adjacent angles are 85° and 95°. Each coordinated water molecule interacts with two DEF molecules by hydrogen bonding (O_{Aqua}–O_{DEF} distances are 2.65 Å and 2.85 Å, respectively). The observed structural parameters such as bonds lengths and angles in this hydrogen-bonded network are in the range of those typically observed for hexaaquazinc complexes.[14d,14e] The only exception is that the Zn–O bond length found here is somewhat shorter than the reported values [the most common Zn–O distances in $Zn(H_2O)_6^{2+}$ complexes are 2.04–2.10 Å] but this could be a problem with accuracy due to the disorder and lowered occupancy.

Other guest molecules, e.g. in smaller channels with the flattened hexagonal cross-section and PSAV of 10%, are highly disordered and the diffuse electron density was corrected by applying the SQUEEZE routine in the PLATON software package.[15]

One can notice that each cluster in TDC-MOF-2 is constructed from two zinc ions and five carboxylic groups, among which three are basal and two are apical. It is unambiguous that the basal groups are negatively charged (deprotonated) carboxylato moieties, whereas the nature of the axial groups is not clear. The charge neutrality of the framework requires that either the pillaring dicarboxylato groups are monoprotonated with the protons disordered over the carboxylato units or that the other crystallographically unresolved positively charged guest species, e.g. diethylammonium, are present in the framework. Three-bladed zinc paddlewheel clusters with axially coordinated nondeprotonated carboxylic groups have, to the best of our knowledge, not been reported up to now[10c] whereas a charge compensation by means of, for example, the alkylammonium cation in pentacarboxylato-di-zinc CU is known.[14f] Our attempts to resolve the structure and nature of the residual guest species in TDC-MOF-2 before SQUEEZE procedures were, nevertheless, unsuccessful. On the other hand, no clear statements about the nature of pillaring TDCs can be drawn by comparison of the structural parameters of the coordination units reported here with those reported in literature data. First, no dinuclear carboxylatozinc CUs, which are structurally and symmetry equivalent to those found in TDC-MOF-2, have been yet described and second, the analysis of data reported on zinc paddlewheel CUs reveals a relatively high flexibility of such structures in terms of geometric parameters. Taking into account all the above, the most plausible stoichiometry for TDC-MOF-2 based on SXRD can, in our opinion, be expressed as $[Zn_2(TDC)_{1.5+x}(HTDC)_{1-x}\cdot[Zn(H_2O)_6]_{x/2}\cdot\{solv\}_y]$, where $x \approx {}^1/_8$ and {solv} represents DEF and any other guests.

Unfortunately, analyses of the TDC-MOF-2 material by TGA, EA and IR spectroscopy does not give enough information to explicitly support the suggested composition, as will be shown below. The TGA-MS data for TDC-MOF-2 measured for the process taking place under argon show

the loss of included solvent molecules in the temperature range 50–250 °C in one broad step, corresponding to an approximately 24% weight loss. The slow weight decrease occurs further as well, followed by a sharp step at ca. 350–360 °C (6.8%) accompanied by a strong increment in MS detection of ions with m/z = 17 a.m.u. The decarboxylation of TDC becomes noticeable at 550 °C (see Figure S10 in the Supporting Information). TGA-MS measurements on the process in a stream of synthetic air indicate the loss of solvent molecules in nearly the same temperature range but the corresponding weight loss is much higher and occurs in two steps (31% at 50–115 °C and 8% at 115–250 °C) which might be due to the differences in the handling of the probes. Additionally, the amount of inorganic remains after burning-out at 400–500 °C is dependant on the batch. This is due to the impurities with a high Zn content e.g. ZnO which are nearly always present in the probes with hexagonal crystals. TGA (synthetic air) of TDC-MOF-2 kept in $CHCl_3$ for several days and subsequently dried in vacuo at 120 °C does not show any weight loss up to 200 °C. At higher temperature a slow decrease of sample mass occurs, followed by burning-out and resulting in 15.3% of residual ZnO ashes. This value is the lowest obtained so far from different TDC-MOF-2 probes.

The PXRD patterns also differ noticeably in the intensities of peaks from batch to batch, as well as upon storage, and this is most probably to do with the amount, location and nature of the guest species remaining in the framework (see Figure S6 in the Supporting Information). Moreover, reflections in the PXRD patterns of TDC-MOF-2 disappear upon drying, indicating the low stability of such a coordination network. No conversion into TDC-MOF-1 seems to take place in this case. The shape of the hexagonal crystals, however, remains unchanged upon drying according to SEM studies (see, for example, Figure S3 in the Supporting Information). We believe that a collapse of the pores in the framework takes place upon guest removal. This would also explain the fact that despite high PSAV, the crystals of TDC-MOF-2 do not soak up chloroform or noticeably exchange the guest molecules against $CHCl_3$ and thus remain swimming on the surface of this solvent, in contrast to other porous MOFs.[16a]

IR spectra of dried TDC-MOF-2 (vac., 120 °C) reveal the presence of aliphatic species in the structure, although a comparison of spectra of the dried and initially synthesised probes indicates that some amount of DEF is removed upon drying (see Figure S9 in the Supporting Information). The residual aliphatic species could be either the coordinated DEF or diethylamine (DEA). The latter might be either coordinated to zinc or form the ion pairs with carboxylic groups of TDC. The elemental analysis of the dried material is unsatisfactory for carbon, however it fits better for coordinated DEF instead of DEA in the structure with the composition $[Zn_2(TDC)_{1.5}(HTDC)\cdot\{ZnO\}_{1/16}\cdot\{DEF\}_2]$. Accounting for the excessive ZnO as an impurity gives an excellent fit of elemental analysis and TGA-data for the composition $[Zn_{16}(TDC)_{12}(HTDC)_8\cdot\{DEF\}_{17}\cdot\{ZnO\}_3]$ (see Exp. Sect.).

Preferential formation of zinc paddlewheel units from dicarboxylic acids and zinc nitrate in DMF under solvothermal synthetic conditions has already been reported.[14a,14b] On the contrary, a series of isoreticular MOFs based on Zn_4O clusters was prepared in DEF by applying similar reaction conditions.[10] Nevertheless, contamination of MOF-5 by other MOF phases was also observed and this appeared to be strongly sensitive to the preparation conditions.[17] The reasons for the unexpectedly dominating Zn_2 paddlewheel assembly by H_2TDC instead of Zn_4O clusters under the conditions of MOF-5 synthesis are not entirely clear and many factors governing this process can be suggested. On the one hand, the bulkiness of triptycene fragments together with their specific symmetry might lead to high steric demands and disturb the 3D self-assembly by means of tetranuclear Zn_4O carboxylato SBUs, although this seems to contradict the preliminary modelling and calculations.[16b] On the other hand, a more efficient spatial arrangement ("gearing") of triptycene fragments in a layered structure such as TDC-MOF-1 can lead to an additional energy gain due to the van der Waals (π-π and CH-π) interactions. The aliphatic nature of the carboxylato groups in H_2TDC in contrast to aromatic –COOH in terephthalic and other acids forming MOFs with Zn_4O coordination units might also play a role in controlling the MOF topology, although some Zn_4O-based structures are also known for aliphatic carboxylato[18a,18b] and carbamato groups.[18c,18d] The mechanism leading to the competitive formation of a hexagonal framework TDC-MOF-2 could not be reasonably established up to now, though our experiments point to the kinetically controlled formation of four-bladed paddlewheel Zn-TDC units, whereas the three-bladed units seem to be preferred thermodynamically.

An interesting feature found from the structural analysis of H_2TDC-based MOFs is the affinity of DEF hydrocarbon residues for the V-shaped clefts of the triptycene moieties composing the frameworks. This observation can be utilised in developing new MOFs for gas uptake with enhanced host-guest interactions. Additionally, the observed tendency of triptycene-dicarboxylic acid to form layered paddlewheel structures with zinc ions can be employed in constructing new porous MOFs using a "pillaring strategy".[14b,19] Based on the pillaring approach, several zinc paddlewheel based MOFs have already been reported, among which that constructed from terephthalic acid and DABCO shows H_2 absorption comparable with MOF-5.[14b,20] Several other dicarboxylato ligands and diamines give analogous assemblies, though often with interpenetration.[14b,21] The latter effect will be, however, unattainable if $Zn_2(TDC)_2$ layers were pillared because of the overlapping triptycene moieties. A possible advantage of such pillared structures created by H_2TDC could be a strongly increased "contact surface" of the 2D layers capable of effectively interacting with guests. Additionally, the layers are impermeable to most small molecules (see Figure 2, e) thus giving the anisotropy in permeability to such crystals which might become attractive for advanced applications. The work in this field continues in our laboratory.

Conclusions

Triptycenedicarboxylic acid (H_2TDC) was applied here for the first time to construct new coordination polymers with zinc ions. Although the solvothermal synthesis in DEF generally resulted, after the respective work-up, in the non-porous 2D MOF based on zinc TDC paddlewheel coordination units, an additional crystalline phase such as small hexagonal columns was also obtained under certain reaction conditions. According to SXRD analysis, it appeared to be a new 3D MOF based on zinc TDC "three-bladed paddlewheels" which possesses relatively big channels filled with guest molecules and might be potentially interesting for studying the guest exchange, removal and binding processes. Additionally, 2D MOFs can be modified using a "pillaring" strategy into porous 3D systems in which the triptycene fragments are expected to enhance the van der Waals interactions between guest molecules and the framework, acting as "clefts" for small molecules.

Experimental Section

General: All chemicals and solvents were purchased from commercial sources and were used without additional purification, unless otherwise mentioned.

Instrumentation: NMR: Bruker AMX400 (400 MHz for ^{1}H and 100 MHz for ^{13}C). IR: Bruker FTIR IFS-113V; IFS-55. Elemental Analysis: Elementar Vario EL. TGA: Mettler Toledo TGA/SDTA 851 (N_2, 50 mL min^{-1}; 10 °C min^{-1}); Netzsch STA 409 PC Luxx coupled with Aeolos QMS 403 C (Ar or synthetic air, 60 mL min^{-1}; 10 °C min^{-1}). BET: Quantachrome Autosorb-1. PXRD: PANalytical X'Pert PRO MPD system; STOE STADI P system with an IP-PSD detector. SEM: Hitachi TM-1000 tabletop microscope; Zeiss DSM 962 electron microscope with EDX equipment from EDAX Boston.

Crystal Structure Determination: The crystal structure determination was carried out on a Xcalibur diffractometer (Oxford Diffraction, Ruby CCD) using Cu-K_α (λ = 1.54178 Å) radiation, osmic mirrors at T = 100 K, with full-sphere data collection omega and phi scans. The CrysAlis programs were used for data collection and reduction. A semiempirical absorption correction using spherical harmonics (SCALE3 ABSPACK algorithm) was applied. Crystal structure solutions were achieved by direct methods and the refinements were carried out on $|F^2|$ against all reflections after merging using the programs implemented in SHELXTL Version 6.10.[22] All non-hydrogen atoms were refined including anisotropic displacement parameters.

One of the COO^- groups in the structure TDC-MOF-2 was refined as a disordered group. The channels in the structure are partly occupied by solvent molecules. Since most of them are highly disordered with no possibility of refining them reasonably, they were removed using the SQUEEZE routine implemented in the software package PLATON.[15] Only one guest molecule of diethylformamide could be reasonably refined in the structure.

CCDC-664462 and -664463 contain the supplementary crystallographic data for this paper. These data can be obtained free of charge from The Cambridge Crystallographic Data Centre via www.ccdc.cam.ac.uk/data_request/cif.

For summary of crystal structure analysis data on TDC-MOF-1 and -2 see Table 2.

Table 2. Summary of crystal and structure refinement data for TDC-MOF-1 and -2.

	TDC-MOF-1	TDC-MOF-2
Empirical formula	$C_{27}H_{23}NO_5Zn$	$C_{41.67}H_{31}NO_{7.75}Zn_{1.38}$
Formula weight	506.83	759.56
Crystal system	monoclinic	hexagonal
Space group	*C*2/*c*	*P*6/*m*
a / Å	16.0157(1)	33.9418(7)
b / Å	14.4722(1)	33.9418(7)
c / Å	21.6977(2)	14.2185(6)
α / °	90.00	90.00
β / °	108.804(1)	90.00
γ / °	90.00	120.00
$V_{calcd.}$ / Å^3	4760.72(6)	14185.8(7)
$\rho_{calcd.}$ / g cm^{-3}	1.414	1.067
Z	8	12
$2\theta_{max}$	65.70	66.04
μ / mm^{-1}	1.752	1.264
(T_{min}/T_{max})	0.90195/1.00000	0.84776/1.00000
Reflections measured	13678	69984
Reflections independent	3974	8562
Restrains/parameters	0/309	4/505
R, wR [$I > 2\sigma(I)$]	0.0247, 0.0673	0.0633, 0.2055
R, wR (all data)	0.0279, 0.0689	0.0705, 0.2175
(ρ_{max}/ρ_{min}) / e Å^{-3}	0.378/–0.238	1.941/–1.159

Synthesis

9,10-Triptycenedicarboxylic acid (H_2TDC): this was prepared from anthracene according to the synthetic pathway proposed earlier.[13] Chloromethylation of anthracene and synthesis of intermediate 9,10-acetoxymethylanthracene were carried out as described elsewhere.[23,24] $C_{22}H_{14}O_4$ (342.4): calcd. C 77.18, H 4.12; found C 77.07, H 4.20. ^{1}H NMR (400 MHz, [D$_6$]DMSO): δ, ppm = 7.12 (m AA′BB′, 6 H), 7.88 (m AA′BB′, 6 H). ^{13}C NMR (100.6 MHz, [D$_6$]DMSO): δ = 61.9 (s), 124.7 (s), 126.4 (s), 144.8 (s), 171.9 (s) ppm. FTIR (KBr): $\tilde{\nu}$ = 3060 (–2520 v. br. medium-intensity peak with multiple weak maxima), 1705 (vs), 1598 (w), 1453 (s), 1405 (m), 1317 (m), 1270 (s), 1215 (w), 1175 (w), 1144 (vw), 1048 (w), 1007 (w), 931 (m), 855 (vw), 772 (w), 754 (s), 684 (m), 642 (m), 606 (w), 524 (w), 480 (m), 440 (w) cm^{-1}. TGA (N_2 stream): weight loss at 360–410 °C (–97%).

TDC-MOF-1 and -2: In a typical procedure, warm (ca. 50 °C) solutions of zinc(II) nitrate tetrahydrate (0.78 g, 3 mmol) in DEF (10 mL) and triptycenedicarboxylic acid (0.344 g, 1 mmol) in DEF (10 mL) were mixed together in a pressure-resistant glass tube, sealed and placed in a block with a programmable thermostat (Barkey Company) preheated to 50 °C. The temperature was gradually raised to 110–120 °C (at 10–20 °C h^{-1}) and kept constant for 15–24 h. The hot reaction mixture was decanted and the resultant crystals covered with fresh solvent. After filtering, the product was dried under vacuum at room or elevated temperature to give TDC-MOF-1.

The decanted reaction solution was placed in a pressure-resistant glass tube, sealed and heated further at 120 °C for several days to yield crystals of TDC-MOF-2 contaminated with an unidentified by-product.

Alternatively, preheated to 120 °C, the reactants (same quantities as in a typical procedure above) were mixed in a pressure-resistant glass tube, sealed and maintained at 120 °C for 8–15 h. An increase of the Zn/H_2TDC ratio resulted in a longer reaction time and improved the appearance of TDC-MOF-2 crystals, though the amount of Zn-containing impurities also increased.

TDC-MOF-1, as-synthesised: $[Zn_2(TDC)_2(DEF)_2]\cdot x DEF\cdot y H_2O$: no reproducible TGA and elemental analysis. For example, for $x = 2$ and $y = 2$: calcd. C 61.40, H 5.80, N 4.47; found C 61.64, H 5.87, N 4.27 (probe A). For $x = 1$ and $y = 1$: calcd. C 62.55, H 5.25, N 3.71; found C 62.54, H 5.22, N 3.48 (probe B). For $x = 0.5$ and $y = 1$: calcd. C 62.70, H 4.98, N 3.24; found C 62.78, H 5.08, N 3.10 (probe C). TGA (N_2, batch 1): weight loss at 90–110 °C (–9.5%; H_2O; $y \approx 6$), 170–190 °C (–0.7%; DEF; $x \approx 0.08$), 270–360 °C (–13.2%), 370–490 °C (–13.1%), 510–620 °C (–22.8%). TGA (N_2, batch 2): weight loss at 90–110 °C (–4.2%; H_2O; $y \approx 2.6$), 170–190 °C (–4.9%; DEF; $x \approx 0.54$), 270–360 °C (–14.0%), 370–490 °C (–12.8%), 510–620 °C (–23.1%).

TDC-MOF-1, dried at 150 °C/vacuum: For $[Zn_2(TDC)_2(DEF)_2]$: calcd. C 63.98, H 4.57, N 2.76; found C 63.11, H 4.61, N 2.66. TGA (N_2): weight loss at 270–360 °C (–13.6%), 370–490 °C (–15.4%), 510–620 °C (–27.4%). FTIR (KBr): $\tilde{\nu}$ = 3054 (vw), 2974 (w), 2934 (w), 2875 (vw), 1665 (sh), 1634 (vs), 1443 (m), 1399 (s), 1361 (sh), 1296 (w), 1264 (w), 1213 (w), 1182 (vw), 1104 (w), 1086 (vw), 1046 (w), 1015 (w), 941 (w), 899 (vw), 814 (m), 759 (w), 745 (m), 712 (m), 691 (w), 646 (w), 626 (m), 494 (vw), 469 (m) cm^{-1}.

TDC-MOF-2, as-synthesised: $[Zn_2(TDC)_{1.5+x}(HTDC)_{1-x}\cdot[Zn(H_2O)_6]_{x/2}\cdot\{solv\}_y]$: no reproducible TGA and elemental analysis. TGA (Ar): weight loss at 50–260 °C (–25%), 260–340 °C (–4%), 340–360 °C (–7%), 360–500 °C (–4%), 500–700 °C (–29%). TGA (synthetic air): weight loss at 50–115 °C (–31%), 115–260 °C (–8%), 260–400 °C (–6%), 400–550 °C (–40%). FTIR (KBr): $\tilde{\nu}$ = 3425 (w), 3062 (w), 2976 (m), 2939 (w), 2875 (vw), 1636 (vs), 1444 (vs), 1400 (vs), 1298 (s), 1265 (m), 1215 (m), 1186 (w), 1164 (w), 1143 (vw), 1116 (w), 1105 (w), 1047 (m), 1016 (w), 943 (w), 902 (vw), 825 (m), 811 (m), 752 (s), 713 (w), 692 (m), 646 (s), 627 (s), 492 (m), (br) cm^{-1}.

TDC-MOF-2, dried at 120 °C/vacuum: For $[Zn_{16}(TDC)_{12}(HTDC)_8\cdot\{DEF\}_{17}\cdot\{ZnO\}_3]$: calcd. C 64.18, H 4.46, N 2.42; ZnO ashes 15.7; found C 64.24, H 4.53, N 2.46; ZnO ashes 15.3. TGA (synthetic air): weight loss at 200–400 °C (–16%), 400–550 °C (–69%). FTIR (KBr): $\tilde{\nu}$ = 3421 (w), 3058 (w), 2979 (w), 2937 (vw), 1622 (vs), 1444 (vs), 1408 (vs), 1296 (s), 1211 (w), 1186 (w), 1163 (w), 1144 (vw), 1086 (vw), 1045 (m), 1016 (w), 941 (w), 902 (vw), 814 (s), 748 (s), 715 (m), 692 (s), 646 (s), 627 (s), 484 (m), (br) cm^{-1}.

Supporting Information (see also the footnote on the first page of this article): including IR spectra, PXRD patterns, TGA plots, photos and SEM pictures of compounds as well as ORTEP plots of asymmetrical units of TDC-MOF-1 and -2.

Acknowledgments

We would like to thank Dr. W. Seidl (Lehrstuhl für Bauchemie, Technische Universität München) for helpful discussions and for help in acquiring of TGA-MS data.

[1] O. R. Evans, R.-G. Xiong, Zh. Wang, G. K. Wong, W. Lin, *Angew. Chem.* **1999**, *111*, 557–559; *Angew. Chem. Int. Ed.* **1999**, *38*, 536–538.

[2] T. M. Reineke, M. Eddaoudi, M. Fehr, D. Kelley, O. M. Yaghi, *J. Am. Chem. Soc.* **1999**, *121*, 1651–1657.

[3] a) M. Fujita, Y. J. Kwon, S. Washizu, K. Ogura, *J. Am. Chem. Soc.* **1994**, *116*, 1151–1152; b) J. S. Seo, D. Whang, H. Lee, S. I. Jun, J. Oh, Y. J. Jeon, K. Kim, *Nature* **2000**, *404*, 982–986; c) C.-D. Wu, A. Hu, L. Zhang, W. Lin, *J. Am. Chem. Soc.* **2005**, *127*, 8940–8941.

[4] a) J. L. C. Rowsell, O. M. Yaghi, *J. Am. Chem. Soc.* **2006**, *128*, 1304–1315; b) J. L. C. Rowsell, O. M. Yaghi, *Angew. Chem.* **2005**, *117*, 4748–4758; *Angew. Chem. Int. Ed.* **2005**, *44*, 4670–4679; c) A. J. Fletcher, K. M. Thomas, M. J. Rosseinsky, *J. Solid State Chem.* **2005**, *178*, 2491–2510.

[5] M. Eddaoudi, D. B. Moler, H. Li, B. Chen, T. M. Reineke, M. O'Keeffe, O. M. Yaghi, *Acc. Chem. Res.* **2001**, *34*, 319–330.

[6] a) J. L. C. Rowsell, A. R. Millward, K. S. Park, O. M. Yaghi, *J. Am. Chem. Soc.* **2004**, *126*, 5666–5667; b) J. L. C. Rowsell, J. Eckert, O. M. Yaghi, *J. Am. Chem. Soc.* **2005**, *127*, 14904–14910; c) M. Hirscher, B. Panella, *Scripta Materialia* **2007**, *56*, 809–812; d) H. Frost, T. Düren, R. Q. Snurr, *J. Phys. Chem. B* **2006**, *110*, 9565–9570.

[7] a) A. L. Grzesiak, F. J. Uribe, N. W. Ockwig, O. M. Yaghi, A. M. Matzger, *Angew. Chem.* **2006**, *118*, 2615–2618; *Angew. Chem. Int. Ed.* **2006**, *45*, 2553–2556; b) N. L. Toh, M. Nagarathinam, J. J. Vittal, *Angew. Chem.* **2005**, *117*, 2277–2281; *Angew. Chem. Int. Ed.* **2005**, *44*, 2237–2241; c) P. D. C. Dietzel, R. Blom, H. Fjellvag, *Dalton Trans.* **2006**, 586–593; d) M. Edgar, R. Mitchell, A. M. Z. Slawin, P. Lightfoot, P. A. Wright, *Chem. Eur. J.* **2001**, *7*, 5168–5175.

[8] a) H. Li, M. Eddaoudi, M. O'Keeffe, O. M. Yaghi, *Nature* **1999**, *402*, 276–279; b) H. Li, C. E. Davis, T. L. Groy, D. G. Kelley, O. M. Yaghi, *J. Am. Chem. Soc.* **1998**, *120*, 2186–2187; c) H. Li, M. Eddaoudi, T. L. Groy, O. M. Yaghi, *J. Am. Chem. Soc.* **1998**, *120*, 8571–8572.

[9] Y. Wang, B. Bredenkötter, B. Rieger, D. Volkmer, *Dalton Trans.* **2007**, 689–696.

[10] a) M. Eddaoudi, J. Kim, N. Rosi, D. Vodak, J. Wachter, M. O'Keeffe, O. M. Yaghi, *Science* **2002**, *295*, 469–472; b) N. W. Ockwig, O. Delgado-Friedrichs, M. O'Keeffe, O. M. Yaghi, *Acc. Chem. Res.* **2005**, *38*, 176–182; c) S. I. Vagin, A. K. Ott, B. Rieger, *Chem. Ing. Technol.* **2007**, *79*, 767–780.

[11] B. Kesanli, Y. Cui, M. R. Smith, E. W. Bittner, B. C. Bockrath, W. Lin, *Angew. Chem.* **2005**, *117*, 74–77; *Angew. Chem. Int. Ed.* **2005**, *44*, 72–75.

[12] a) N. Kulevsky, K. Pierce, *Spectrochim. Acta Part A: Mol. and Biomol. Spectrosc.* **1993**, *49*, 417–423; b) A. Furlan, S. Leutwyler, M. J. Riley, *J. Chem. Phys.* **1994**, *100*, 840–855.

[13] B. H. Klanderman, J. W. H. Faber, patent, FR 1520625, **1968**, 9 pp.

[14] a) H. F. Clausen, R. D. Poulsen, A. D. Bond, M.-A. S. Chevallier, B. B. Iversen, *J. Solid State Chem.* **2005**, *178*, 3342–3351; b) H. Chun, D. N. Dybtsev, H. Kim, K. Kim, *Chem. Eur. J.* **2005**, *11*, 3521–3529; c) M. Edgar, R. Mitchell, A. M. Z. Slawin, P. Lightfoot, P. A. Wright, *Chem. Eur. J.* **2001**, *7*, 5168–5175; d) P. Knuuttila, *Polyhedron* **1984**, *3*, 303–305; e) J. W. Steed, B. J. McCool, P. C. Junk, *J. Chem. Soc., Dalton Trans.* **1998**, 3417–3423; f) J. Klunker, M. Biedermann, W. Schafer, H. Hartung, *Z. Anorg. Allg. Chem.* **1998**, *624*, 1503–1508.

[15] a) P. van der Sluis, A. L. Spek, *Acta Crystallogr., Sect. A* **1990**, *46*, 194–201; b) A. L. Spek, *J. Appl. Crystallogr.* **2003**, *36*, 7–13.

[16] a) A. Ott, S. Vagin, B. Rieger, unpublished results. b) R. Schmid, S. Amirjalayer, personal communications on the unpublished results.

[17] A. L. Grzesiak, F. J. Uribe, N. W. Ockwig, O. M. Yaghi, A. J. Matzger, *Angew. Chem. Int. Ed.* **2006**, *45*, 2553–2556.

[18] a) W. Clegg, D. R. Harbron, C. D. Homan, P. A. Hunt, I. R. Little, B. P. Straughan, *Inorg. Chim. Acta* **1991**, *186*, 51–60; b) H. Koyama, Y. Saito, *Bull. Chem. Soc. Jpn.* **1954**, *27*, 112–114; c) A. Belforte, F. Calderazzo, U. Englert, J. Straehle, *Inorg. Chem.* **1991**, *30*, 3778–3781; d) C. S. McCowan, T. L. Groy, M. T. Caudle, *Inorg. Chem.* **2002**, *41*, 1120–1127.

[19] a) S. Kitagawa, M. Kondo, *Bull. Chem. Soc. Jpn.* **1998**, *71*, 1739–1753; b) G. Ferey, *Chem. Mater.* **2001**, *13*, 3084–3098.

[20] D. N. Dybtsev, H. Chun, K. Kim, *Angew. Chem.* **2004**, *116*, 5143–5146; *Angew. Chem. Int. Ed.* **2004**, *43*, 5033–5036.

[21] B.-Q. Ma, K. L. Mulfort, J. T. Hupp, *Inorg. Chem.* **2005**, *44*, 4912–4914.
[22] G. M. Sheldrick, Universtität Göttingen (Germany), **2000**.
[23] M. W. Miller, R. W. Amidon, P. O. Tawney, *J. Am. Chem. Soc.* **1955**, *77*, 2845–2848.
[24] T. Nakaya, T. Tomomoto, M. Imoto, *Bull. Chem. Soc. Jpn.* **1966**, *39*, 1551–1556.

Received: December 12, 2007
Published Online: April 23, 2008